Canadian Science Publishing | **Canadian Journal of Civil Engineering**

Dynamic Characteristics of Light-Frame Wood Buildings

SCHOLARONE™
Manuscripts

1   # Dynamic Characteristics of Light-Frame Wood Buildings

2   Ghazanfarah Hafeez[1], Ghasan Doudak[2], Ghyslaine McClure[3]

3   **ABSTRACT**

4   This paper deals with dynamic field testing of light-frame wood buildings with wood based shear

5   walls. The primary objective of the investigation is to provide an estimate of the fundamental

6   period of such buildings, through field testing and numerical modelling. An experimental program

7   is established to perform ambient vibration testing on forty-one light-frame wood buildings of both

8   regular and irregular layouts, located in moderate to high seismic zones in different regions in

9   Canada. The research objective is to develop a reliable method of estimating the building period

10   of light-frame wood buildings and develop an accurate expression for building period estimate

11   based on field testing and numerical modeling. The study found that significant scatter is observed

12   in the measured data when plotted as a function of building height. Finite element models were

13   developed and compared with the natural periods of the buildings with reasonable accuracy. Using

14   the validated FE models to examine different commonly used stiffness models showed that in

15   general current analysis approaches overestimate the building period.

16   Keywords: Timber structures; lateral drift; fundamental building period; stiffness; light frame

17   wood buildings.

[1] PhD Candidate, Department of Civil Engineering, University of Ottawa, 161 Louis-Pasteur, Ottawa, ON K1N 6N5

[2] Associate Professor, Department of Civil Engineering, University of Ottawa, 161 Louis-Pasteur, Ottawa, ON K1N 6N5

[3] Professor, Department of Civil Engineering and Applied Mechanics, McGill University, 817 Sherbrooke Street West, Montréal, Québec, Canada, H3A 0C3

1

18   **INTRODUCTION**

19   **LIGHT- FRAME WOOD BUILDINGS**

20   Light-frame wood structures represent about 90% of the construction industry in North America,

21   where the majority of this construction type consists of low-rise residential and commercial

22   occupancies (Raineri et al. 2006). The expected performance of such buildings of normal

23   importance is that the safety of occupants is preserved under any loading conditions including

24   extreme event of natural catastrophes such as strong wind and earthquakes. In a typical light-frame

25   wood structure, the main types of structural components that resist lateral loads are horizontal floor

26   and roof diaphragms and vertical shear walls. The floor diaphragm is typically a system of equally

27   spaced joists covered with structural sheathing and fastened mechanically to the storey below or

28   the concrete foundation wall by anchor bolts. A shear wall (Figure 1) is an assembly of bottom

29   and top plates, vertical studs and sheathing, designed to resist the horizontal load effects. Floor or

30   roof elements are typically attached to the top plates of the shear walls using mechanical fasteners.

31   The vertical elements (studs) of shear walls are connected with structural sheathing, such as

32   oriented strand board (OSB) or plywood, through nails. The floors are connected together using

33   anchorages and the end studs of the shear walls are attached with discrete or continuous hold-down

34   connections. Roofing consists of prefabricated truss elements, covered with sheathing and attached

35   to the exterior of the top chord of the trusses. For more information on construction details of light-

36   frame wood buildings the reader is referred to documents such as CMHC (2014).
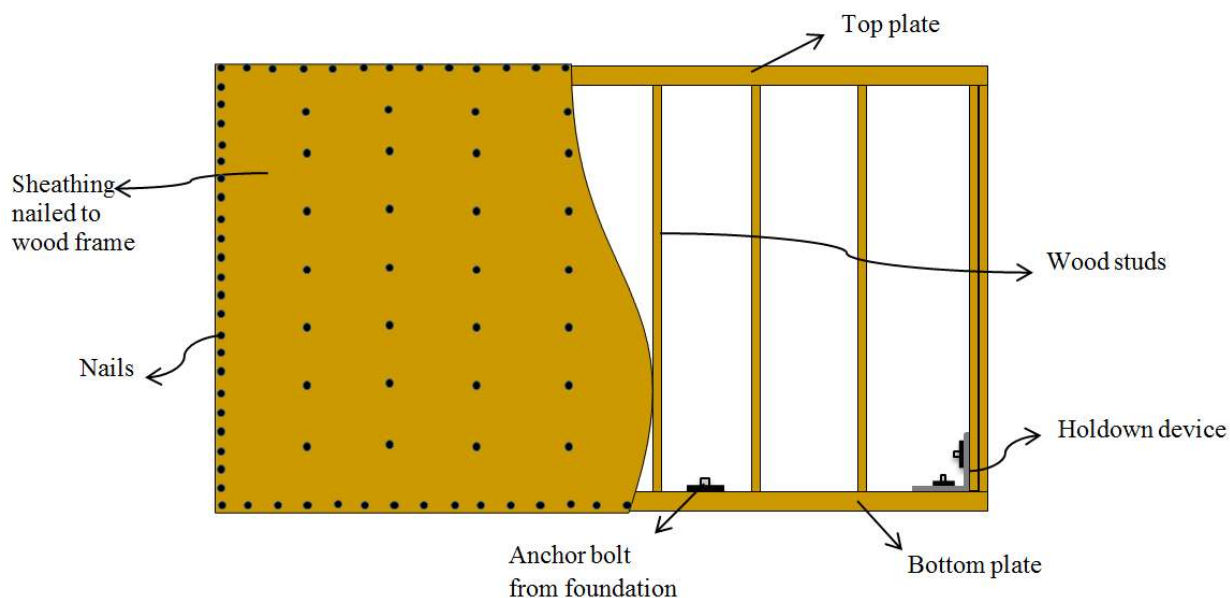
37 **Figure 1: Sketch of a shear wall**

38

39 **DYNAMIC BEHAVIOR OF LIGHT- FRAME WOOD BUILDINGS**

40 The behavior of a building during an earthquake is determined by the characteristics of the ground

41 shaking (intensity and frequency content) and the dynamic properties of the building's lateral load

42 resisting system, namely its natural frequencies, mode shapes, and damping ratios. These dynamic

43 parameters are difficult to estimate accurately before the structure is built, and it is, therefore

44 necessary to make certain simplifying design assumptions to determine them. The National

45 Building Code of Canada (NBCC) specifies design seismic ground motions as five percent-

46 damped uniform hazard acceleration spectra (UHS) and provides a simple empirical formula,

47 shown in Equation (1), to estimate the fundamental period as a function of building height for

48 preliminary design (NRC 2015).

3

$$T = 0.05(h_n)^{0.75} \tag{1}$$

49   The general accuracy of Equation (1) is uncertain considering that it has not been calibrated to

50   light-frame wood buildings. The current research is motivated to support a more rational design

51   approach by establishing reliable guidelines to assess the fundamental period and lateral stiffness

52   of wood buildings based on a suitable database of field tests.

53   The dynamic charecteristics of timber buildings have been investigated by several studies where

54   measurement methods like ambient vibration, force vibration, and shaketable tests have been

55   employed. Kharrazi (2001, 2006) conducted a research study on low-rise timber buildings with

56   emphasis on vibration behavior using different vibration methods. Ambient vibration and

57   sinusoidal tests were carried out on the house specimens before and after the earthquake motion

58   simulations to observe the decrease in natural frequency resulting from the stiffness degradation

59   (damage incurred) during testing. The study established a correlation between ambient and forced

60   vibration test results for correcting the period measured by ambient vibration testing. Equation (2)

61   was proposed by the authors for low levels of excitation. F_V and F_{AV} in Equation (2) are the forced

62   vibration and ambient vibration frequencies, respectively.

$$F_V = 0.65(F_{AV})^{1.1} \tag{2}$$

63   Ellis and Bougard (2001) performed dynamic testing on a six-storey timber building in three

64   different construction stages. Details about the building construction are provided in Enjily and

65   Palmer (1998). The objective of the study was to determine the racking stiffness from measured

66   fundamental modes of vibration of bare frame and completed building. In the finished structure,

4

67   measurements performed using ambient and forced vibration methods confirmed that

68   measurements taken during forced vibration tests produced smaller frequencies than those from

69   ambient vibrations, however the difference between the two test methods was deemed small. The

70   seismic performance of a two-storey wood frame house was evaluated on a reduced scale uni-axial

71   shake table at the University of California, San Diego (Filiatrault et al. 2002). Ambient vibration

72   testing was performed before and after each seismic test, to determine the effect on fundamental

73   period and mode shapes of the test structure. The study concluded that the roof displacement was

74   decreased by more than a factor of three due to increasing in lateral stiffness of the structure

75   incorporating the wall finishing materials. The mean damping ratio increased with the addition of

76   the wall finishes. Camelo (2003) studied the vibration behavior of wood based buildings by

77   developing a database of dynamic properties, such as natural frequencies, damping ratio and mode

78   shapes of the structures. A two-storey house at UC San Diego and a three-storey building with

79   tuck-under parking at UC Berkley were tested at different phases of construction. The study

80   showed a strong dependence of the period on the amplitude, and proposed a period formula as a

81   function of building height (in feet) shown in Equation (3), to represent the behavior of wood

82   buildings, which was compared with the period formula provided in Uniform Building Code

83   (UBC-97).

$$T = 0.032(h_n)^{0.55} \hspace{5cm} (3)$$

84   Christovasilis et al. (2008) performed full-scale testing on a tri-axial shake table to study the

85   parameters that influence the seismic behavior of light-frame wood buildings. The research

86   concluded that finishing material increased the lateral stiffness and consequently reduced the

87   displacement response of the building. Full-scale shake table testing was performed on a six-storey

88   light wood frame apartment building (Van de Lindt et al. 2010). The structure was designed

89   according to performance-based seismic design procedure and the goal of the test was to determine

90   parameters such as building fundamental period, base shear, inter-storey drifts, acceleration, and

91   hold-down forces. Multiple seismic tests were performed and the natural period of the building

92   was identified before and after every test. Although the floor plan of the building was

93   approximately symmetric and the seismic masses were evenly distributed, torsional response was

94   observed during the seismic test. Some visible damage, limited to only non-structural components

95   were noticed.

OBJECTIVES

96

97   The above review highlights the need to systematically investigate the dynamic parameters that

98   influence the behaviour of light frame wood buildings of different configurations. The current

99   study attempts to contribute to this area by developing and analyzing a large database of dynamic

100   characteristics of light frame wood buildings across Canada. The overarching goal of this research

101   project is to develop a reliable method of estimating the building period of light-frame wood

102   buildings. More specifically the study aims to develop an accurate expression for building period

103   estimate based on field testing and numerical modeling. The adequacy of contemporary code

104   formula for estimating the fundamental period of timber buildings, specifically those consisting of

105   light-frame wood shear walls, is evaluated. The essential elements that define the research

106   methodology are ambient vibration field testing, analysis of recorded measurements, and stiffness

107   estimation of lateral load resisting system. Numerical building models are developed and validated

108   with the data obtained from field testing. The validated models are then used to evaluate different

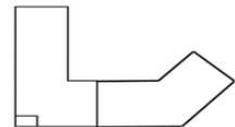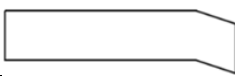109   stiffness models used to estimate the fundamental periods of light frame wood buildings.
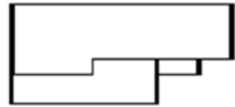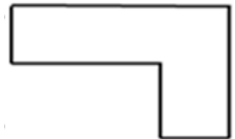
Experimental Program
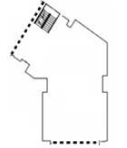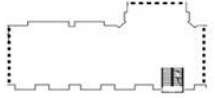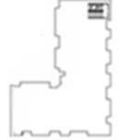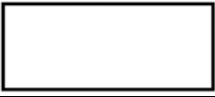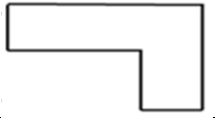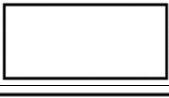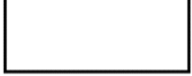
111   The dynamic properties of a structure, such as its natural frequencies, corresponding mode shapes

112   and damping ratios, can be obtained by a number of experimental methods including forced

113   vibration, free vibration, and ambient vibration testing (AVT). AVT has become a popular and

114   practical experimental method for assessing the dynamic behavior of full-scale structures mainly

115   because of its non-destructive nature and its simplicity, where the building is excited by ambient

116   operational loads (e,g, wind and traffic), whether under construction or in use. In AVT, the

117   excitation forces on the structure are undefined (assumed white noise), and the modal properties

118   are obtained from the measured response only; this is also known as output-only modal

119   identification. Additional practical advantages of AVT are that the preliminary results are available

120   shortly after each test run and testing can be performed on different sizes and types of structures.

121   The low amplitude ambient vibration method has, for several decades, been used to study the

122   change in dynamic characteristics of a structure at various construction stages (e.g. Schuster et al.

123   (1994); Skrinar and Strukelj (1996); Ventura and Schuster (1996)) and different excitation levels
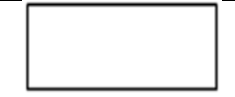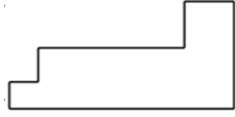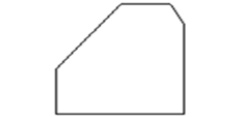
124   (e.g. Gates (1993); Ivanovic et al. (2001); Beck et al. (1994a)).
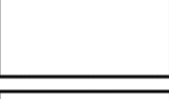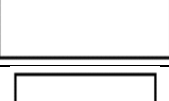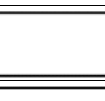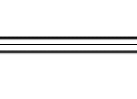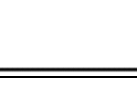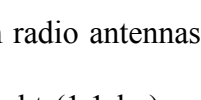
125   An experimental program was established to perform AVT on forty-one (41) light-frame wood

126   buildings of both regular and irregular layouts and located in moderate to high seismic zones in

127   different regions in Canada. All measured buildings consist of residential occupancies. The

128   locations, heights and plan geometries of all tested buildings are provided in Table 1.

129   **Table 1: Geometric details of measured buildings**

Building ID	Location	No. of Storeys	Height (m)	Length (m)	Width (m)	Geometry
B1	Kamloops, BC	5W+1C +B[1]	17.4	70	40	

B2	Kamloops, BC	5W+1C +B	17.4	89	70	
B3	Kamloops, BC	5W+1C +B	18.2	184	20	
B4	Quebec city, QC	6w	18	51.8	19.9	
B5	Kamloops, BC	4W+1C	18.1	60	24	
B6	Orleans, ON	4W+B	14.2	44	16.5	
B7	Ottawa, ON	4W+B	14.9	65	33	
B8	Vancouver, BC	4W+B	14.9	25	17	
B9	Fredericton, NB	4W+B	13.6	51.4	41	
B10	Okanagan, BC	5W	16	30	12	
B11	Okanagan, BC	4W+1C	16	35	31	
B12	Vancouver, BC	3W+2C	20.2	55	26	
B13	Kamloops, BC	2W+3C	16	28	24	

B14	Kingston, ON	4W +B	14.3	80	18	
B15	Kingston, ON	4W +B	14.3	57	18	
B16	Kingston, ON	4W +B	14.3	18	45	
B17	Kingston, ON	4W +B	14.3	50	34	
B18	Kingston, ON	4W +B	14.3	52	24	
B19	Kingston, ON	4W +B	16.79	52	32	
B20	Kingston, ON	3W +B	15.8	51	30	
B21	Kingston, ON	3W +B	15.8	26	15	
B22	Ottawa, ON	3W +B	12	20	9	
B23	Ottawa, ON	3W +B	11.83	18.7	9.4	
B24	Ottawa, ON	3W +B	11.83	18.7	9.4	
B25	Ottawa, ON	3W +B	10.11	15	12	
B26	Orleans, ON	3W +B	12.3	36	18	
B27	Orleans, ON	3W +B	12.3	18	15	

9

B28	Ottawa, ON	3W +B	12.3	18	15	
B29	Ottawa, ON	3W +B	12.3	18	15	
B30	Ottawa, ON	2W +B	6.4	20	7.6	
B31	Orleans, ON	4W	14.28	50	24	
B32	Orleans, ON	4W	14.28	41	24	
B33	Orleans, ON	3W +B	13.1	18	15	
B34	Orleans, ON	3W +B	13.1	18	15	
B35	Boucherville, QC	2W	6	9.7	9.4	
B36	Longueuil, QC	2W	6	9.1	6.7	
B37	Brossard, QC	2W	6	8.5	7.3	
B38	Brossard, QC	2W	6	9.7	9.4	
B39	Brossard, QC	2W	6	9.1	7.3	
B40	Brossard, QC	1W	3	10.3	8.5	
B41	Kamloops, BC	4W	3	70	50	

130   *W, C and B represent wood, concrete and basement, respectively.

131

132 **INSTRUMENTATION**

133 Instrumentation used for AVT comprises of wireless sensors equipped with radio antennas. The

134 sensors have a compact portable size (100mm x 140mm x 8mm) and weight (1.1 kg) and are

135 equipped with four soft-touch keys that enable the user to input required sensing parameters such

10

136   as record duration, sampling rate, and partition numbers. The acquisition frequency range is (0.1-

137   256) Hz, which suffices to include all significant natural frequencies of the building in relation to

138   its overall wind and seismic response. Each sensor is equipped with three orthogonal

139   electrodynamic velocimeters and three orthogonal digital accelerometers. The sensor stores data

140   in an internal memory card and data can be transferred to a personal computer using a USB cable

141   and an interface software (S.P.A. 2008). A sensor is connected to a radio antenna that enables

142   synchronization among the sensors through radio communication. Radio synchronization of

143   sensors with the amplifiers depends on indoor and outdoor locations and physical obstacles. In

144   principle, synchronization among each couple of sensors is possible at a distance up to 400 m.

145   Various sensor layouts were configured according to the building geometry to obtain the

146   fundamental mode shape of each building in two orthogonal directions. One reference sensor (at

147   fixed location) and multiple roving sensors were used for each measurement setup. The ambient

148   response vibrations were recorded for eight minutes in each setup at a sampling frequency of

149   128Hz, which allowed sufficient downscaling of the data and record length for accurate modal

150   extraction. Figure 2 provides four examples of typical sensor configurations. In the case of L-shape

151   buildings, the floor measurements were recorded on both wings of the buildings to capture the

152   fundamental mode shapes corresponding to both extensions.

a)   b)

c)   d)

✳ **Roving sensor**

★ **Reference sensor**

153
154
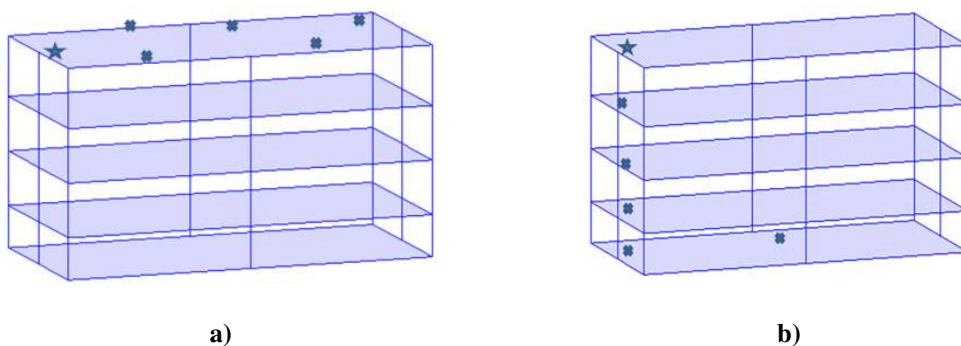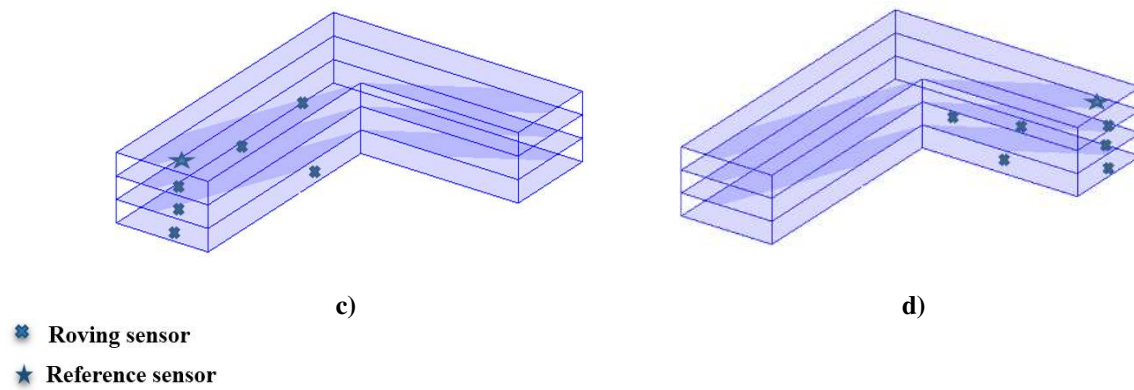
155   **Figure 2: Typical sensor configurations for regular (a, b) and irregular shape (c, d) buildings**

156

157   **Extraction of Modal Parameters**

158   Fundamental natural frequencies and mode shapes of the tested buildings were analyzed by the

159   enhanced frequency domain decomposition (EFDD) technique using the ARTeMIS Extractor

160   software (Structural Vibration Solutions A/S 2011). Recorded horizontal velocity-time histories

161   were treated with autocorrelation functions, which were then transformed to frequency domain to

162   generate power spectral density (PSD) matrices. The spectral densities between each pair of

163   measured records is computed and stored in spectral density matrices. Singular value

164   decomposition (SVD) is performed on each (PSD) matrix and transforms it into three matrices as

165   presented in Equation (4) (Schott 2005).

$$[G] = [U][S][V]^H \tag{4}$$

166   Where [G] is PSD matrix at each frequency, [S] denoted singular value matrix and [U] and [V] are

167   unitary matrices containing orthonormal, left and right singular vectors respectively. H denotes

168   Hermitian transform.

12

169   For each PSD matrix the singular value decomposition is performed giving n sets of singular

170   vectors (represent an approximation to mode shapes) and singular values of an individual

171   frequency (for each setup). The singular values from each measured configuration are averaged

172   across n different measured configurations by normalizing the area under preceding singular value

173   curve. The averaging operation is performed individually for each singular value, as expressed in

174   Equation (5).

$$\{S_i(\omega)\} = \frac{1}{n}\sum_{m=1}^{n} S_i(\omega, m) \tag{5}$$

175   Where i=1,2,3, m is measurement configuration (sensor setup).

176   As shown in Figure 3, averaged singular values are plotted against frequency to offer potential

177   peaks for identification of the building's natural frequencies excited by ambient sources. A single-

178   degree-of-freedom (SDOF) bell shaped function is produced for each measured configuration, by

179   considering all frequencies in the vicinity of a potential peak (resonance frequency) with a singular

180   vector with a high Modal Assurance Criterion (MAC), which defines a measure of consistency

181   (correlation) between two vectors.

Enhanced Frequency Domain Decomposition - Peak Picking
Average of the Normalized Singular Values of Spectral Density
Matrices of all Test Setups
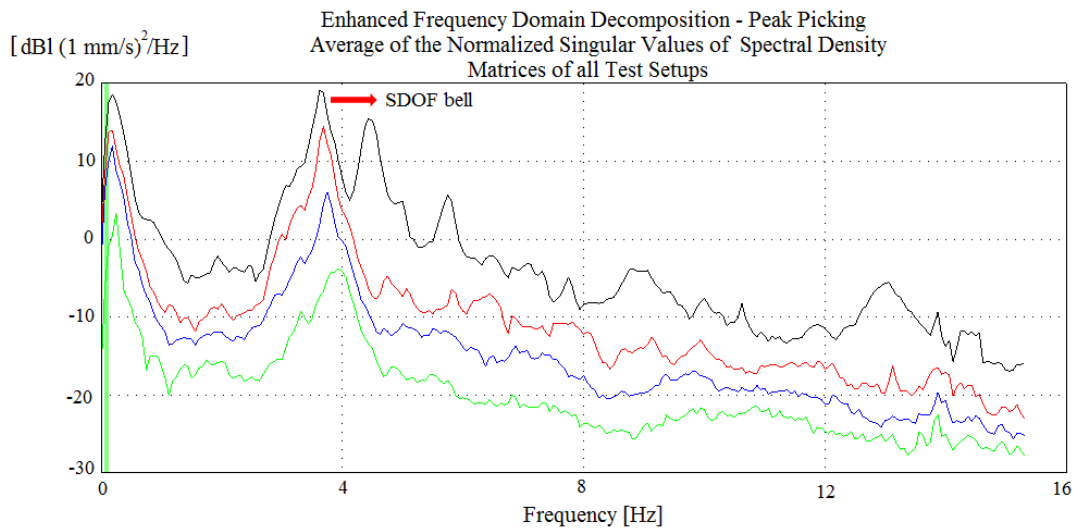
182 **Figure 3: Singular value plot showing SDOF bell-shaped function, building B11**

183

184 **Experimental Results**

185 Table 2 summarizes the fundamental periods and damping ratios obtained for the individual light-

186 frame wood buildings tested. Properties that could not be identified due to faulty reading or missing

187 signals following the processing of AVM records are shown as hyphen "-" in the table. Although

188 two significant digits are provided for damping ratios in the tables, such values are deemed very

189 approximate due to simplifying assumptions in the record analysis. It should be emphasized that

190 the study is not focusing on damping characteristics of wood structures. From Table 2, it can be

191 observed that the frequency range for all tested buildings is 9.1 to 2.2 Hz (0.11-0.46s), and the

192 range found for damping ratios was 1.0-7.3 %.

193 An example of the fundamental mode shapes analyzed in ARTeMIS Extractor (Structural

194 Vibration Solutions 2011) for a regular shape and an L shape buildings can be seen in Figure 4

195 and Figure 5 respectively.

196 **Table 2: Measured natural periods and damping ratios of wood-frame buildings**

Building ID	Natural Period (s)		Estimated Modal Damping Ratio (%)	
	Transverse	Longitudinal	Transverse	Longitudinal
B1	0.20	0.29	-	6.0
B2	0.29	0.31	2.3	2.9
B3	0.46	0.35	3.8	2.7
B4	0.37	0.29	2.5	1.8
B5	0.28	0.35	4.5	5.5
B6	0.20	0.19	4.3	2.4
B7	0.25	0.23	4.6	3.1
B8	0.40	0.25	2.3	2.2
B9	0.20	0.19	3.7	-
B10	0.26	0.23	-	1.5
B11	0.22	0.27	2.4	2.2
B12	0.29	0.32	2.1	2.3
B13	0.32	0.19	4.7	4.1
B14	0.33	0.23	1.4	3.2
B15	0.31	0.29	2.2	4.6
B16	0.29	0.27	2.3	3.3
B17	0.27	0.22	2.1	4.0
B18	0.24	0.19	3.4	-
B19	0.23	0.18	1.2	1.4
B20	0.23	0.26	1.0	-
B21	0.27	-	1.4	-
B22	0.18	0.14	3.1	4.6
B23	0.21	0.23	1.1	3.7
B24	0.35	0.29	1.9	1.1
B25	0.20	0.17	1.8	1.5
B26	-	0.24	-	2.6
B27	0.29	0.23	1.4	3.2
B28	0.26	0.29	-	1.1
B29	0.26	0.32	3.3	2.2
B30	0.20	0.12	1.9	1.3
B31	0.20	0.16	2.2	1
B32	0.21	0.16	1.7	3.8
B33	0.22	0.28	5.7	-

15

B34	0.24	0.28	3.6	-
B35	0.13	-	-	-
B36	0.15	-	7.3	-
B37	0.14	-	-	-
B38	0.12	-	4	-
B39	0.17	-	3.4	-
B40	0.11	-	-	-
B41	-	0.26	-	2.3

197

Transversal mode, (T= 0.20s)   **Longitudinal mode, (T= 0.19s)**
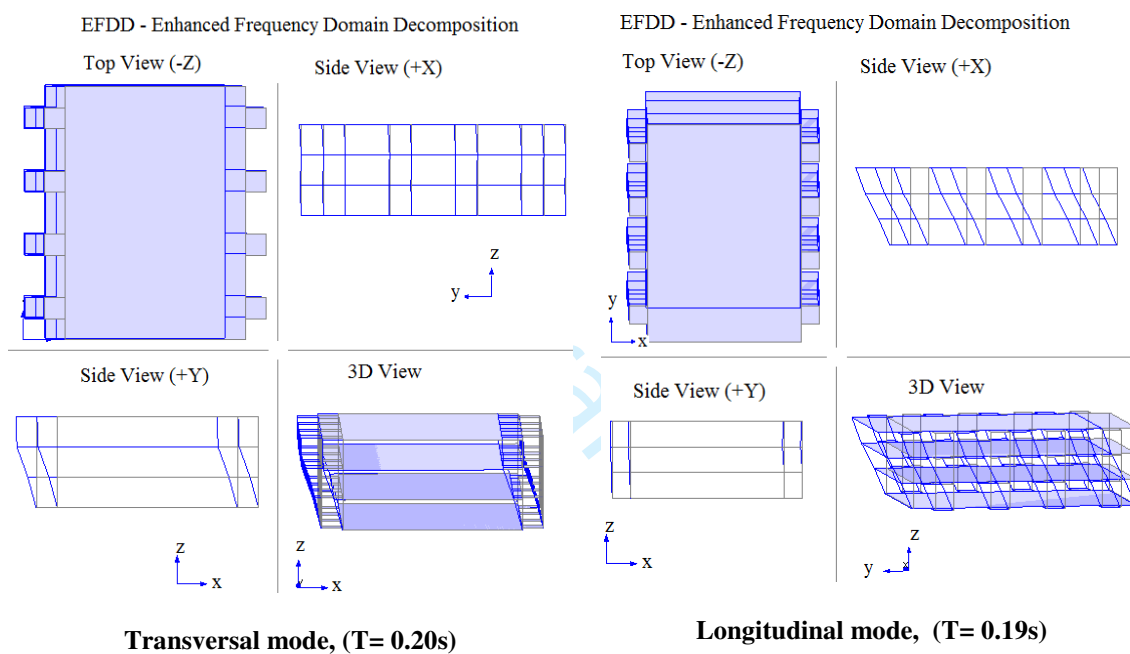
198   **Figure 4: Mode shapes of B8 (Regular shape)**

Transversal Mode, (T= 0.20s)

Longitudinal Mode, (T= 0.29s)
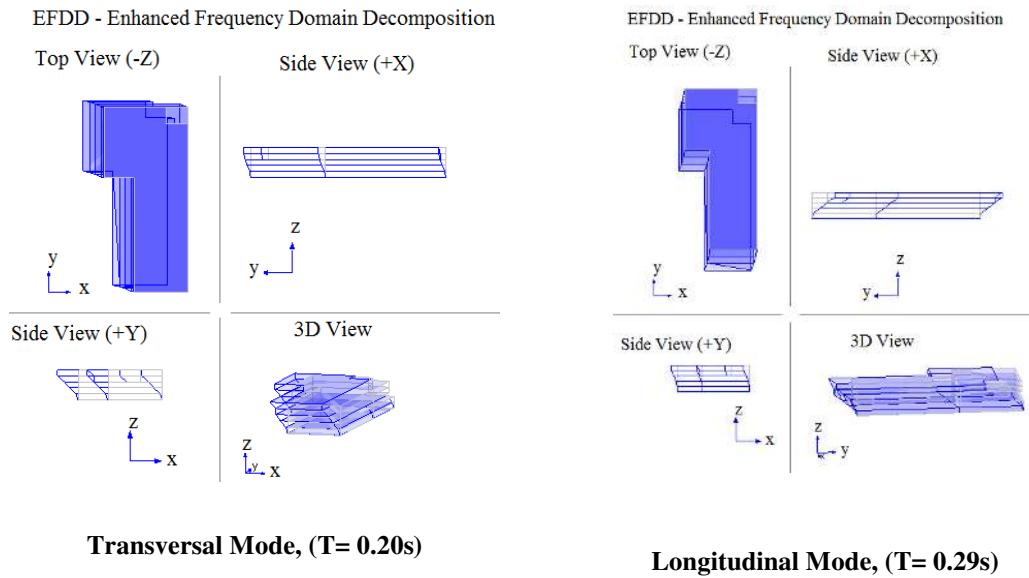
199   **Figure 5: Mode shapes of B1 (Irregular shape)**

200   As indicated in Table 2, the fundamental periods of all measured buildings were extracted in both

201   the longitudinal and transverse directions. In seismic design it is typical to provide the same shear

202   wall capacity and stiffness in the two orthogonal directions since the seismic base shear is a

203   function of the building mass and the period governing the seismic motion. However due to

204   differences in geometry, it is anticipated that the building would be designed with different

205   horizontal stiffness values and therefore different natural periods in the two main directions. The

206   measured period results as a function of building height (in meters) are plotted in Figure 6. Height

207   is chosen here because it is typically the only variable used to describe building periods in building

208   codes (e.g. NBCC (2015); ASCE (2005); BSSC (2003); SEAOC (1999)). Significant scatter is

209   observed in the measured data, which clearly indicates that relying on the building height alone is

210   not sufficient to provide accurate fundamental period estimates. From Figure 6 it can be seen that

211   the periods in the two main directions of the finished buildings are within the same range with no

212   distinctive distinction between the two directions.

17
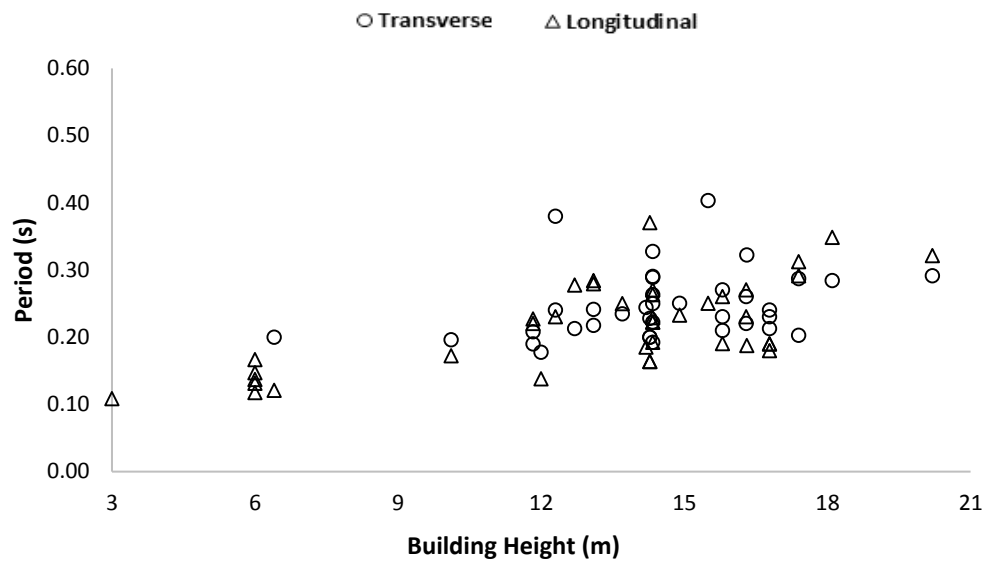
Figure 6: Measured fundamental period vs. building height

213

214   The fundamental periods measured in the current study (AV) together with test results collected

215   from the literature for ambient vibration (AV), forced vibration (FV), and shake table (ST) tests

216   are plotted against building height in Figure 7. As expected, the wide scatter in the data persists.

217   The data points collected during the current study seem indistinguishable from those obtained from

218   the literature, especially from AV testing. Also, the NBCC period equation (Equation (1)) seems

219   to provide a very rough average estimate of the measured data. The data seems to cluster around

220   the building code equation especially for low rise buildings (1-2 storey), whereas for taller

221   buildings the scatter is significantly larger.

222   With a few exceptions, the data measured using AVT (including those from the current study)

223   produce lower period values than those measured during forced vibration or shake table

224   simulations. The difference is especially pronounced for taller buildings due to softening of the

225   lateral load resisting system by increasing the amplitude of shaking. This observation is consistent

226   with the expectation that the fundamental period of a structure increases with the excitation

227   amplitude (e.g. Udwadia and Trifunac (1974)) due to decrease in lateral stiffness (softening

228   behavior) as the amplitude of lateral displacement increases and causes damage and/or nonlinear

229   response.
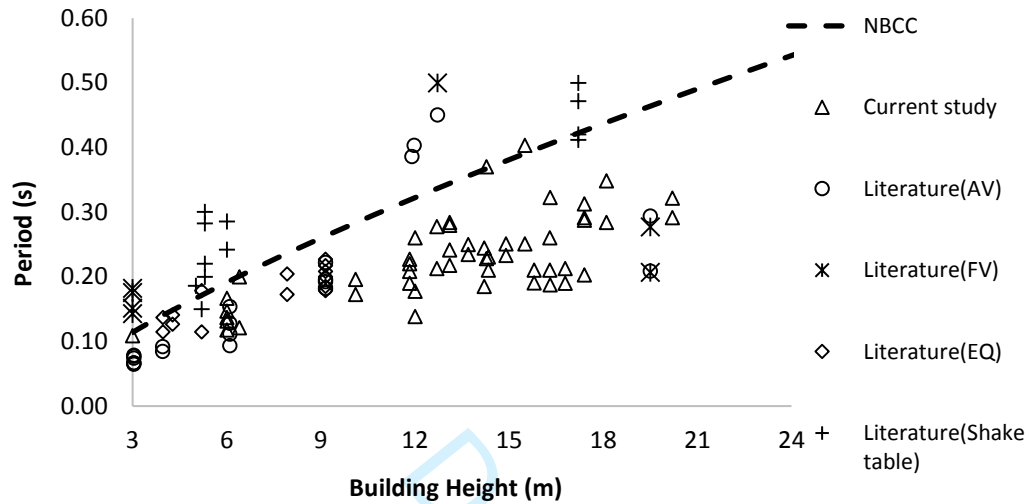
230   **Figure 7: Fundamental periods available in the literature and from current study vs. building height**

231   The results from the current study were also compared to Equation (3), an expression developed

232   by Camelo (2003) as a function of building height (in feet), based on data obtained during low

233   level earthquake shaking and (FV) test results.
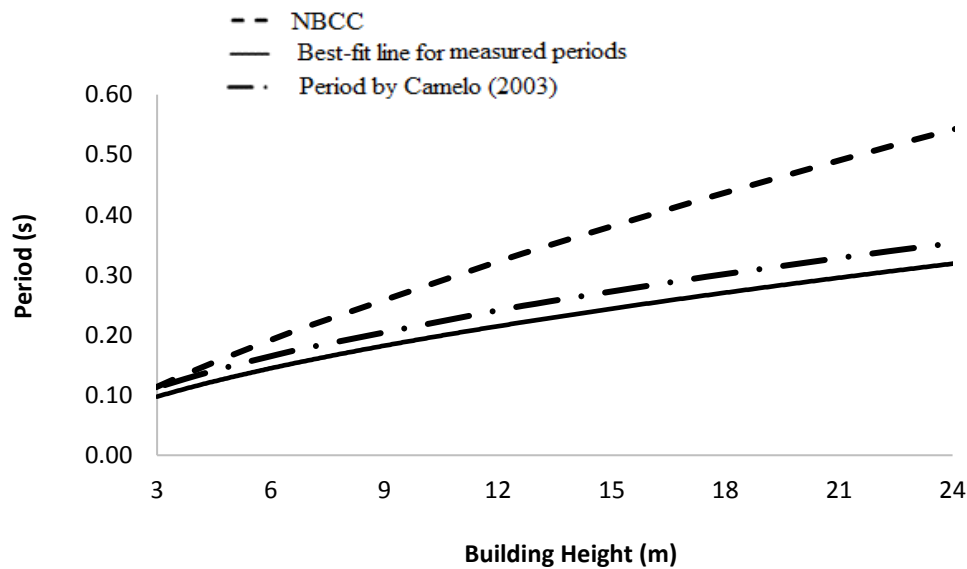
234   **Figure 8: Comparison of fundamental periods obtained from NBCC equation, Equation (3) and AVM test**
235   **data from current study**

236   Figure 8 shows that the equation proposed by Camelo (2003) provides slightly higher period values

237   than those obtained from the current study using AVT. This is expected because the expression by

238   Camelo (2003) is based on FVT and measurements recorded at low amplitude shaking. The periods

239   calculated using the NBCC equation yield significantly higher values than those extracted from

240   AVM tests and obtained from Camelo's (2003) formula.

241   Figure 9 presents the best fit line of the data from the current study modified using Equation (2).

242   The modified curve lies between the ambient vibration measurements and the NBCC formula,

243   which seems reasonable provided that the data were modified for a low level excitation. The

244   proposed trend line is on average a more suitable expression for estimating the period for seismic

245   design, however more work is needed to address the spread in data as observed in Figure 8.

246
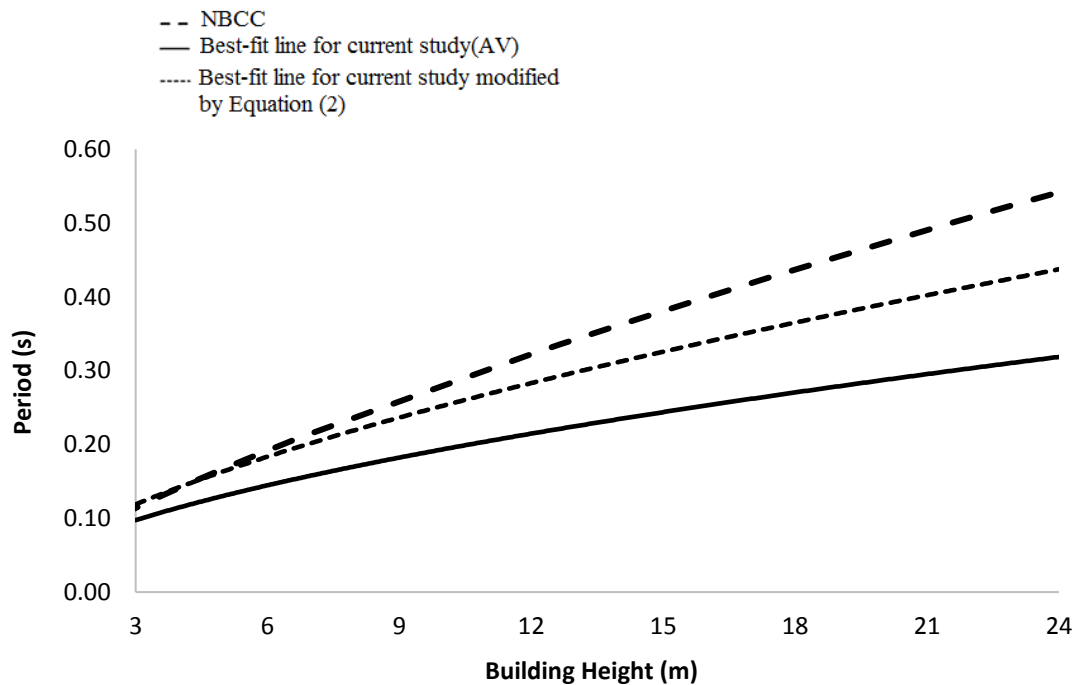
Figure 9: Comparison of fundamental periods obtained from NBCC equation, Equation (2) and AVM test data from current study

249   The difficulty in comparing any level of vibration testing with the NBCC expression stems from

250   the fact that the NBCC equation is not defined for a specific level of loading or vibration amplitude.

NUMERICAL MODELING

252   Several studies have used numerical analysis models to mimic the performance of light-frame

253   wood buildings at a system and component levels with varying levels of complexity (e.g. Gupta

254   and Kuo (1987); Tarabia and Itani (1997); Folz and Filiatrault (2004a, 2004b); Collins et al.

255   (2005a, 2005b); Doudak et al. (2005); Casagrande et al. (2015)). In the current study, selected

256   buildings were modeled in detail using the commercially available software SAP2000®

257   (Computers and Structures 2016). The choice of these buildings was made based on the availability

258   of construction details and structural drawings. Simplified 3D linear elastic models were created

259   for the multi-storey buildings tested in order to determine the fundamental sway period in each

21

260   orthogonal geometric direction. It is assumed that the structure is pinned at its base support, and

261   the floor diaphragms are assumed to be rigid. The building mass was lumped at each floor level.

262   Shear walls were modeled using horizontal links, as shown in Figure 10.
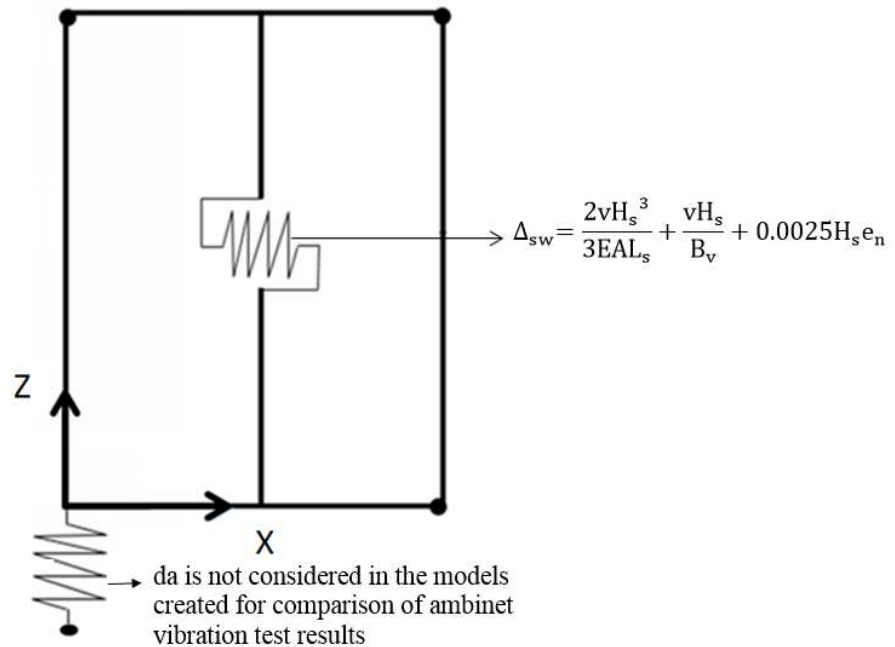
Figure 10: Typical shear wall mode

264   The in-plane lateral stiffness of the wood shear walls was estimated using the deflection equation

265   provided in the Canadian timber design standard, CSA O86 Engineering Design in Wood (CSA

266   2014), reproduced in Equation (6). Omitted from the equation for the purpose of comparison with

267   AVT level results is the contribution from the overturning (4th term in Equation (6)) because it was

268   assumed that at very low level of loading the contribution would be insignifianct given the

269   relatively high gravity load component compared to the horizontal load.

$$\Delta_{sw} = \frac{2vH_s{}^3}{3EAL_s} + \frac{vH_s}{B_v} + 0.0025H_s e_n + \frac{H_s}{L_s}d_a \qquad (6)$$

270 Where Δ_{sw} is the total lateral in-plane deflection, v is applied shear force per unit width length

271 (N/mm), H_s is wall height (mm), E is the modulus of elasticity of end studs (MPa), A is the cross-

272 sectional area of end studs (mm^2), L_s is the length of shear wall segment (mm), B_v is the through-

273 thickness shear rigidity of the sheathing panel (N/mm), and d_a is the horizontal deflection due to

274 wall anchorage details such as rotation and slip at hold-down connections (mm).

275 e_n is the nail slip (in mm) at a particular load per nail and calculated as per Equation (7).

$$e_n = \left[\frac{0.013vs}{d_f^2}\right]^2 , \tag{7}$$

276 where v represents shear force per unit length (N/mm), s is the nail spacing (in mm) at panel edges

277 of shear wall, and d_f is the nail diameter (mm).

278 e_n values for gypsum wall board were obtained using the exponential empirical model equation

279 for joints fastened with screws developed by Lafontaine and Doudak (2017) as expressed in

280 Equation (8).

$$e_n = (4.92 - 0.42\gamma_{GWB})\left[\frac{0.016v_f}{d_s^{1.33}}\right]^{5.5} \tag{8}$$

281 where γ_{GWB} is the gypsum wall board density and d_s is the fasteners' diameter. v_f is the load

282 per fastener (N).

283 The fundamental period results obtained from the numerical building models were validated using

284 the ambient vibration field results. For this purpose, the initial stiffness of a shear wall, $K_{(0-10)\%}$,

285 was determined as 0-10 % slope on the capacity-deflection curve generated using Equation (6). A

286 simplified 3D linear elastic model of building B22 is shown in Figure 11.
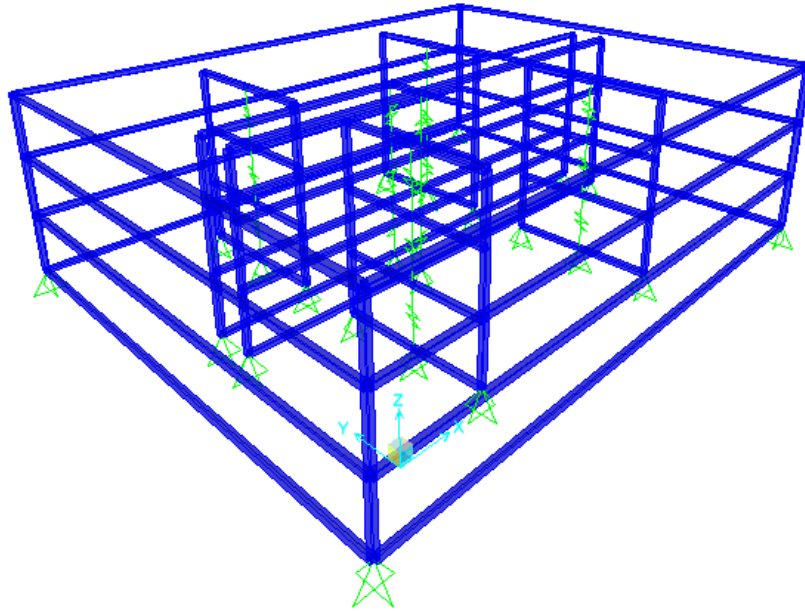
287 **Figure 11: 3D model of building B22**

288 Figure 12 compares the fundamental periods obtained from the numerical models with those from

289 AVT records. It is seen that the computed period slightly overestimates the building period

290 obtained from AVT. This is expected since the estimate of the building reactive mass is anticipated

291 to be fairly accurate, whereas the lateral stiffness is usually underestimated in numerical models.

292 Models describing stiffness, especially at low load level (e.g. AVT), lack the ability to include

293 effects such as friction in connections, the contribution of lintels above and below opening, return

294 walls, etc.

295 In general, larger differences between the periods obtained from numerical models and measured

296 data were observed for irregular shape buildings.
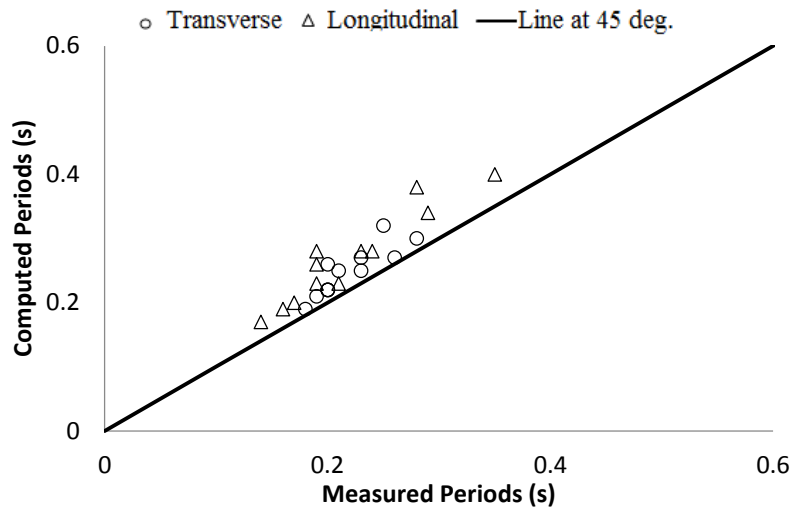
Figure 12: Measured periods vs. model periods

297

298   The validated model was used to investigate two different stiffness models (SM1 and SM2).

299   Stiffness model SM1 is generated using all four terms of Equation (6) while in model SM2 the

300   stiffness is calculated by incorporating the effect of both cumulative frame bending, and the

301   rotational effects from lower stories (CSA 2014; Newfield and Wang 2016). For model SM2, the

302   first and last terms of Equation (6) were modified as shown in Equation (9) and Equation (10),

303   repectively.

$$\Delta_{b,i} = \left[\frac{M_{i+1}H^2}{2(EI)_i} + \frac{V_i\,H^3}{3(EI)_i}\right] + H_i\left(\sum_1^{i-1}\theta_j\right) \tag{9}$$

304   Where, M_i is overturning moment, V_i is the inter-story shear force, $(EI)_i$ is the total bending rigidity

305   of the shear wall under consideration, and θ_j is the angle between tangents to the elastic deflection

306   curve at the bottom and top of the ith storey.

$$\Delta_{hd,i} = H_i \alpha_i + H_i \left(\sum_1^{i-1} \alpha_j \right) \qquad (10)$$

307   Where, $\alpha_i = (d_a)_i / L_s$ for small angles and $(d_a)_i$ is the total vertical elongation of the wall

308   anchorage system at the ith story.

309

310   The designer is likely to estimate the buidling period using design level forces while using the

311   SM2 model as suggested by the design standard (CSA 2014). In the models used in the current

312   paper, the stiffness was conservatively assume to be the 10-40 % slope on the capacity-deflection

313   curve. It is assumed that this approach would be conservative because it would yield higher

314   stiffness estimate than that computed using design level forces. In Figure 13, the computed periods

315   using models SM1 and SM2 are compared to those provided by Equation (1), as well as the upper

316   limit (twice the period by Equation (1)) required by the code (NRC 2015).

317

318   The results in Figure 13 show that model SM1 (with no cummulative effects) is at or slightly above

319   the NBCC period, calculated using Equation (1). It should be noted that the NBCC buidling period

320   represented a reasonable average estimate for tests conducted using shaketable and high level

321   forced vibration testing (Figure 7) and that it was higher than what was obtained from AVT and

322   low level FVT (Figure 8). The fact that period values calculated using model SM2 significantly

323   exceeds the emperical code period and in some cases even exceeds the upper limit of the NBCC

324   equation shows that the current seismic analysis approaches (those involving design level forces

325   and cummulative effects) may lead to and overestimation of the building period. In fact in some

326   cases the period value using SM2 exceeds the upper limit of the NBCC. Although directed by the

327   code to limit the period at twice the value obtained from Equation (6), the observed trend indicates

26

328 that calculated base shear design estimates may be non-conservative as seismic demand decreases

329 when the period is increased.
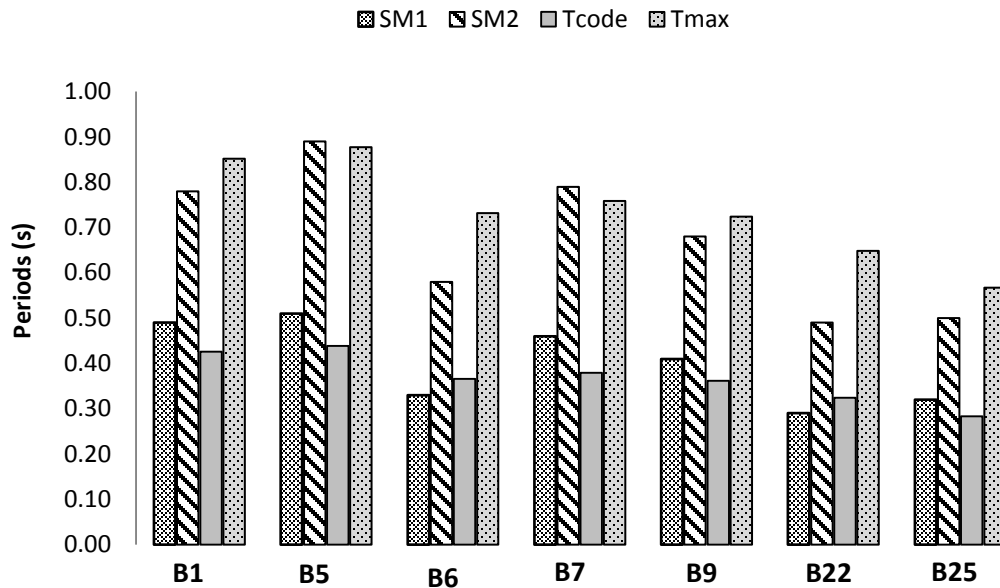
330

Figure 13: Comparison between computed and code periods

331 Future research by the authors aims at developing more reliable expressions based on the collected

332 data that would reduce the variability and provide estimates of the building period that will better

333 reflect the dynamic characteristics of light-frame wood buildings.

334 **Conclusion**

335 A comprehensive data base of measured dynamic properties of light-frame wood building has been

336 compiled based on ambient vibration tests. The measured buildings include a variety of geometries

337 and occupancies. The extracted results include fundamental natural frequencies, and

338 corresponding damping ratios and mode shapes, of the measured buildings. Specifically, the

339 following conclusions can be drawn from the current study:

27

340   -   Significant scatter is observed in in the measured data as a function of building height. This

341   clearly indicates that relying on the building height alone to describe the building period is

342   not sufficient to provide accurate estimates.

343   -   The periods obtained from the current study are consistent with those reported in the

344   literature for ambient vibration measurements. Data obtained through shake table and

345   forced vibration testing show higher period values, which can be attributed to the increase

346   in excitation amplitude.

347   -   FE models were developed and their ability to capture the period and mode shapes

348   observed in the experimental study was investigated. The results showed that the FE

349   models were able to predict the natural periods of the buildings with reasonable accuracy

350   while the computed period slightly overestimates the building period obtained from AVT.

351   Larger differences between the periods obtained from the numerical models and measured

352   data were observed for irregular shape buildings and for those which are interconnected

353   with firewall separations.

354   -   Using the validated FE models to examine commonly used stiffness models showed that

355   in general current analysis approaches may overestimate the building period, with some

356   cases even exceeding the upper limit defined by the NBCC.

357

References

358 **References**

359 ASCE. 2005. Minimum design loads for buildings and other structures (ASCE/SEI 7-05).

360 Structural Engineering Institute, American Society of Civil Engineers, Reston, VA, U.S.A.

361 BSSC. 2003. NEHRP recommended provisions for seismic regulations for new buildings and other

362 structures (FEMA 450), Building Seismic Safety Council, National Institute of Building

363 Standards, Washington, D.C.

364 Beck, J., L., May, B., S., and Polidori, D., C. 1994a. Determination of modal parameters from

365 ambient vibration data for structural health monitoring. *In* Proceedings of First World Conference

366 on Structural Control, International Association for Structural Control, Los Angeles, California,

367 U.S.A., pp. TA3-3.

368 Casagrande, D., Rossi, S., Sartori, T., & Tomasi, R. 2015. Proposal of an analytical procedure and

369 a simplified numerical model for elastic response of single-storey timber shear-walls. Construction

370 and Building Materials, 102: 1102-1112.

371 Canadian Standards Association (CSA) 2014. CAN/CSA O86-14 Engineering design in wood,

372 Ontario, Canada.

373 Computers and Structures, I.C., SAP 2000-advanced, 2014.

374 CHMC, 2014. Canadian wood frame house construction. 3rd ed, Canada Mortgage and Housing

375 Corporation, Canada.

376 Christovasilis, I. P., Filiatrault, A., and Wanitkorkul, A. 2008. Seismic testing of full scale wood

377 structures on two shake tables. World Conference on Earthquake Engineering, Beijing, China.

378   Collins, M., Kasal, B., Paevere, P., & Foliente, G., C. 2005. Three-dimensional model of light

379   frame wood buildings. I: Model description. Journal of Structural Engineering, 131(4): 676-683.

380   Collins, M., Kasal, B., Paevere, P., & Foliente, G., C. 2005. Three-dimensional model of light

381   frame wood buildings. II: Experimental investigation and validation of analytical model. Journal

382   of Structural Engineering, 131(4): 684-692.

383   Camelo, V., S. 2003. Dynamic characteristics of wood frame buildings. Doctoral dissertation,

384   California Institute of Technology, Pasadena, California, U.S.A.

385   Doudak, G., McClure, G., Smith, I., Hu, L., & Stathopoulos, T. 2005. Monitoring structural

386   response of a wooden light-frame industrial shed building to environmental loads. Journal of

387   structural engineering, 131(5): 794-805.

388   Ellis, B., R., and Bougard, A., J. 2001. Dynamic testing and stiffness evaluation of a six-storey

389   timber framed building during construction. Engineering Structures, 23(10): 1232-1242.

390   Enjily, V., Palmer, S. 1998. TF2000-Background and progress of fullscale testing. *In* 3rd

391   Cardington Conference, UK.

392   Folz B, Filiatrault A. 2004a. Seismic analysis of woodframe structures, I: Model formulation.

393   Journal of Structural Engineering, 130(9):1353–60.

394   Folz B, Filiatrault A. 2004b. Seismic analysis of woodframe structures, II: Model implementation

395   and verification. Journal of Structural Engineering, 130(9):1361–70.

396   Filiatrault, A., Fischer, D., Folz, B., and Uang, C., M. 2002. Seismic testing of two-story

397   woodframe house: Influence of wall finish materials. Journal of Structural Engineering, 128(10):

398   1337-1345.

399   Gates, J., H. 1993. Dynamic field response studies and earthauqke instrumentation of the meloland

400   road overcrossing. In Structural Engineering in Natural Hazards Mitigation, American Society of

401   Civil Engineers, 343-348.

402   Gupta, A., K., and Kuo, G., P. 1987. Modeling of a wood-framed house. Journal of Structural

403   Engineering, 113(2): 260-278.

404   Ivanovic, S., S., Trifunac, M., D. and Todorovska, M., D. 2001. On identification of damage in

405   structures via wave travel times. Strong Motion Instrumentation for Civil Engineering Structures,

406   Springer, Netherlands, 447-467.

407   Kharrazi, M. H., & Ventura, C. E. 2006. Vibration frequencies of woodframe residential

408   construction. Earthquake spectra, 22(4): 1015-1034.

409   Kharrazi, M., H., K. 2001. Vibration characteristics of single-family woodframe building. Master

410   thesis, University of British Columbia, Vancouver, Canada.

411   Lafontaine, A., Chen, Z., Doudak, G., & Chui, Y. H. 2017. Lateral behavior of light wood-frame

412   shear walls with gypsum wall board. Journal of Structural Engineering, 04017069.

413   Newfield, G., Wang, J. 2016. A comparative analysis of three methods used for calculating

414   deflections for multi-storey wood shearwalls, World Conference on Timber Engineering, Vienna,

415   Austria.

416   NRC/IRC. 2015. National Building Code of Canada 2015. National Research Council of Canada,

417   Institute for Research in Construction, Ottawa, Ontario.

418   Rainer, J. H., Ni, C., Cheng, H., Follesa, M. and Karacabeyi, E. 2006. Research program on the

419   seismic resistance of conventional wood-frame construction.In Proceedings of the 8th U.S.

420   National Conference on Earthquake Engineering, San Francisco, California, USA, pp 1203.

421   Structural Vibration Solutions A/S. 2011, ARTeMIS Extractor Handy (Version 5.3) [Software],

422   Available from http://www.svibs.com.

423   S.P.A., M., Manuale tromino ENG TR-ENGY PLUS October 2008, M. S.P.A., Editor 2008.

424   Schott, J., R. 2005. Matrix analysis for Statistics. Willey &Sons, Hoboken, New Jersey, U.S.A.

425   SEAOC. 1999. Recommended lateral force requirements and commentary (SEAOC Blue Book).

426   Seismology Committee, Structural Engineers Association of California, Sacramento, CA.

427   Skrinar, M., and Strukelj, A. 1996. Eigenfrequency monitoring during bridge erection. Structural

428   Engineering International, 6(3): 191-194.

429   Schuster, N., D., Ventura, C., E., Felber, A., and Pao, J. 1994. Dynamic characteristics of a 32-

430   story high-rise building during construction. *In* 5th US National Conference on Earthquake

431   Engineering, Chicago, Illinois, US.A., pp. 701-710.

432   Tarabia, A., M., & Itani, R., Y. 1997. Seismic response of light-frame wood buildings. Journal of

433   Structural Engineering, 123(11): 1470-1477.

434   Udwadia, F., E., and Trifunac, M., D. 1974. Time and amplitude dependent response of structures.

435   Earthquake Engineering and Structural Dynamics, *2*(4): 359-378.